PCCP

This is an *Accepted Manuscript*, which has been through the Royal Society of Chemistry peer review process and has been accepted for publication.

Accepted Manuscripts are published online shortly after acceptance, before technical editing, formatting and proof reading. Using this free service, authors can make their results available to the community, in citable form, before we publish the edited article. We will replace this *Accepted Manuscript* with the edited and formatted *Advance Article* as soon as it is available.

You can find more information about *Accepted Manuscripts* in the Information for Authors.

o-Benzyne fragmentation and isomerization pathways. A CASPT2 study.

Giovanni Ghigo,* Andrea Maranzana, Glauco Tonachini

Dipartimento di Chimica, Università di Torino, via P. Giuria 7-10125 Torino

Abstract: The mechanisms of the fragmentation and isomerization pathways of *o*-benzyne have been studied at the multi-configurational second-order perturbative level CAS(12,12)-PT2. The direct fragmentation of *o*-benzyne to C_2H_2 + C_4H_2 follows two mechanisms: a concerted one (already subject to several studies) and a stepwise, studied here with the appropriate method for the first time. While the concerted mechanism is characterized by a single closed shell transition structure, the stepwise pathway is more complex and sees structures with strong diradical character. A third diradicaloid fragmentation pathway of *o*-benzyne yields, as final product, C_6H_2.

Alternatively to fragmentations, *o*-benzyne can undergo to rearrangements to its *meta* and *para* isomers and to the open-chain *cis* and *trans* isomers of hexa-3-en-1,6-diyne (HED). These are found to easily fragment to C_2H_2 + C_4H_2 or C_6H_2.

The kinetic modelling, performed at several temperatures (800 - 3000 K), found that the thermal decomposition of *o*-benzyne is predicted to yield C_2H_2, C_4H_2 and C_6H_2 as main products. Small amounts of HEDs can accumulates only below 1200 K because they rapidly decompose. Between 1000 and 1400 K, C_2H_2 + C_4H_2 form exclusively from decomposition of *trans*-HED. Above 1400 K, C_2H_2 + C_4H_2 also form from the direct fragmentation of *o*-benzyne. The formation of C_2H_2 + C_4H_2 prevails up to 1600 K then, above this temperature, the formation of C_6H_2 prevails. However, above 2400 K, the direct fragmentation of *o*-benzyne makes the formation of C_2H_2 + C_4H_2 to prevail, again. The formation of hydrogen atoms is also justified.

KEYWORDS: Benzyne, diacetylene, acetylene, hexatriyne, hydrogen, CASPT2

Introduction

The formation of 1,2-didehydrobenzene, also known as *o*-benzyne (*o*-C_6H_4),[1] was first proposed in 1927 by Bachmann and Clarke.[2] Due to its nature of extremely reactive species, *o*-C_6H_4 was isolated in matrix and spectroscopically characterized by Chapmann only in 1973.[3] Later, other vibrational spectra have been registered[4,5,6] and calculated.[7,8] The structural parameters for *o*-C_6H_4 have been obtained by microwave experiments only in the early 2000s.[9,10,11,12] The latest computational work appeared last year[13] testifying the interest for this molecule.

o-Benzyne, for which several synthetic thermal routes have been described,[14] shows a remarkably diverse chemistry[15] and finds applications in organic synthesis.[16,17] *o*-C_6H_4 is also an important intermediate formed in the pyrolysis of benzene whose thermal decomposition takes place in fuel combustion and industrial reforming for olefin production. It has been proved, in fact, that the main decomposition channel for C_6H_6 passes through a C-H fissions first yielding the phenyl radical[18,19] then *o*-C_6H_4 through a second C-H fission[20,21,22] or through a hydrogen transfer in a self-reaction between phenyl radicals.[23,24] Recent studies proposed a ~~potential~~ role of *o*-benzyne for the formation of PAHs in the combustion of aromatic fuels.[22,25,26,27] In particular, there are indications that *o*-C_6H_4 could be a key factor in the formation of multi-ring intermediates in phenyl radical pyrolysis.[28,29,30] It has also been suggested that *o*-C_6H_4 could be present

in the inter-planetary *nebulae*[31] and have a role in the formation of PAHs in the interstellar chemistry.[32] The pyrolysis of benzene and aromatics can, of course, proceed beyond *o*-benzyne, which can gives rise to further fragmentations and isomerizations. The simplest fragments that the thermal decomposition of this molecules can originate are acetylene C_2H_2 and but-1,3-diyne (diacetylene) C_4H_2. For this reaction, a concerted mechanism was first proposed.[33] This concerted mechanism was reported in other works[22,34,35,36] and only in 2011[37] an alternative stepwise pathway was proposed.[38] In 1999 Moskaleva *et al.*[34] included in their model for the thermal decomposition the isomerization to *meta*- and *para*-benzyne and the ring opening to hexa-3-en-1,6-diyne. Later on, alternative mechanisms for the rearrangements were put presented.[39,40,41] In their investigation on the production of hydrogen atoms in the thermal dissociation of *o*-C_6H_4 Xu *et al.*[36] included in their model, along with the fragmentation to C_2H_2 + C_4H_2, also the H-elimination (but not the isomerizations). At the present, all models used to describe the thermal fragmentation of *o*-benzyne to C_2H_2 + C_4H_2 include the concerted mechanism but not the stepwise mechanism and the theoretical methods chosen cannot take properly in account the diradical nature of some species (whatever intermediate or transition structure). Moreover, no one includes all pathways, *i.e.* the fragmentations to C_2H_2 + C_4H_2 and to C_6H_3 + H, the isomerizations to *meta*- and *para*-benzyne, or the ring opening to hex-3-en-1,6-diyne. In this work we presents the results of the kinetic study at different pyrolysis temperatures (800 – 3000 K) based on thermochemical data obtained through the study of the potential energy surface (PES) calculated at the multi-configurational second-order perturbative level (CASPT2). This method will allow us to properly and homogeneously describe all structures originated in the pathways cited above, included those with diradical electronic structure. The kinetic model is based on the *Boltzmann* distribution of energy and it is valid whatever method *o*-benzyne is generated. All data useful for alternative treatments (*e.g.* RRKM) are reported in the Supporting Information.

Results and Discussion

In this work (see Method section for details) all structures are first optimized at the CASSCF which allow us the calculation of the vibrational frequencies then structures are re-optimized at the CASPT2 level to get reliable energy values. These are then combined with the CASSCF ZPE to get the final energy values. Their difference with respect to *o*-benzyne are reported in Tables and commented in the text.

Concerted *vs.* stepwise fragmentation pathways of *o*-benzyne. In their study, Zhang *et al.*[35] assumed that the fragmentation of *o*-benzyne and some derivatives takes place through a concerted mechanism. However, they also suggested that the reaction could ~~also~~ take place with a stepwise mechanism but they did not investigate any further. Therefore, in the present work we explore the whole potential energy surface (PES), both at the CASSCF and CASPT2 level, to find out all stationary points, either intermediates or first-order (TS) or second-order (SOSP) saddle points, whose structures are reported in Scheme 1 and energies in Table 1. We first identified the concerted transition structure **TS$_C$** at 89.8 kcal mol^{-1} that immediately yields C_2H_2 + C_4H_2 (55.7 kcal mol^{-1}). The calculated energy barrier values is close to that one reported by previous studies[34,35,37] performed with single-reference methods. This is not surprising because this transition structure only shows a small diradical character. The weight of the closed

shell *aufbau* configuration (*i.e.* $(C_0)^2$) at the CASSCF level is 78%. This corresponds to occupation numbers close to the typical closed shell values (2 or 0): the most diverging values are 1.89 and 0.11. These values can be compared, *e.g.*, to 1.92 and 0.09 in diacetylene (the occupation numbers for all structures are reported in the Supporting Information). The structure (Figure 1, left) also is similar to that found in the cited papers.

The stepwise pathway is more complex being characterized by a CC bond breaking followed by a sequence of *s-cis/s-trans* and *cis/trans* interconversions which terminate with the final CC bond breaking that yields the fragments C_2H_2 + C_4H_2. The first step is the ring opening through **TS$_1$** (Figure 1, right) located at 85.9 kcal mol^{-1} (3.9 kcal mol^{-1} below **TS$_C$**). **TS$_1$** shows a diradical nature being the weight of the *aufbau* configuration 52%. This corresponds to occupation numbers far away from the typical closed shell values (2 or 0): the relevant values are 1.27 and 0.73. The correct description of the diradical nature of **TS$_1$** is fundamental: Ayaz *et al.*[37] obtained an energy difference of this TS with respect to **TS$_C$** of only 0.7 kcal mol^{-1} (*i.e.* too low compared to our 3.9).

The intermediate generated by **TS$_1$** is the *s-cis* diradical **I$_t$** located at 85.5 kcal mol^{-1}. From this intermediate two conformational isomerization pathways open: the *cis/trans* **TS$_2$** (85.8 kcal mol^{-1}) involving a displacement of the vinyl hydrogen *gem* to the radical centre and leading to diradical **I$_c$** (83.3 kcal mol^{-1}) and the *s-cis/s-trans* **TS$_3$'** (87.1 kcal mol^{-1}) consisting in the rotation of the vinyl radical moiety and leading to the *s-trans* diradical **II$_t$** (82.9 kcal mol^{-1}). Diradical **I$_c$** isomerizes through the *s-cis/s-trans* **TS$_3$** (83.0 kcal mol^{-1}) to the diradical **II$_c$** (79.3 kcal mol^{-1}) which can also be formed through the *cis/trans* **TS$_2$'** (83.5 kcal mol^{-1}) from the diradical **II$_t$**. Intermediate **II$_c$** is the most stable diradical intermediate and finally leads to the fragments C_2H_2 + C_4H_2 through the second CC bond breaking in **TS$_4$** (83.7 kcal mol^{-1}). In this transition structure the diradicaloid nature starts to fade out because it leads to closed shell products; the weight of the *aufbau* configuration is 73% and the occupation numbers of the relevant molecular orbitals are 1.74 and 0.26. A stationary point corresponding to the CC bond breaking of radical **I$_c$** was find on the CASSCF potential energy but it resulted to be a second order saddle point (**SOSP** in Scheme 1). The analog CC bond breaking transition structures from intermediates **I$_t$** and **II$_t$** do not exist. All attempts to optimize their structures lead to **TS$_3$** or **SOSP**. Therefore, starting from diradical **I$_t$**, both pathways requires *s-cis/s-trans* and *cis-trans* isomerizations and involve structures (**I$_t$, I$_c$, II$_t$, II$_c$, TS$_2$, TS$_2$', TS$_3$,** and **TS$_3$'**) that are diradicals (the occupation numbers of the relevant molecular orbitals are close to 1). The pathway **I$_t$** - **I$_c$** - **II$_c$** (first towards right then down in Scheme 1) is slightly energetically preferred (Table 1).
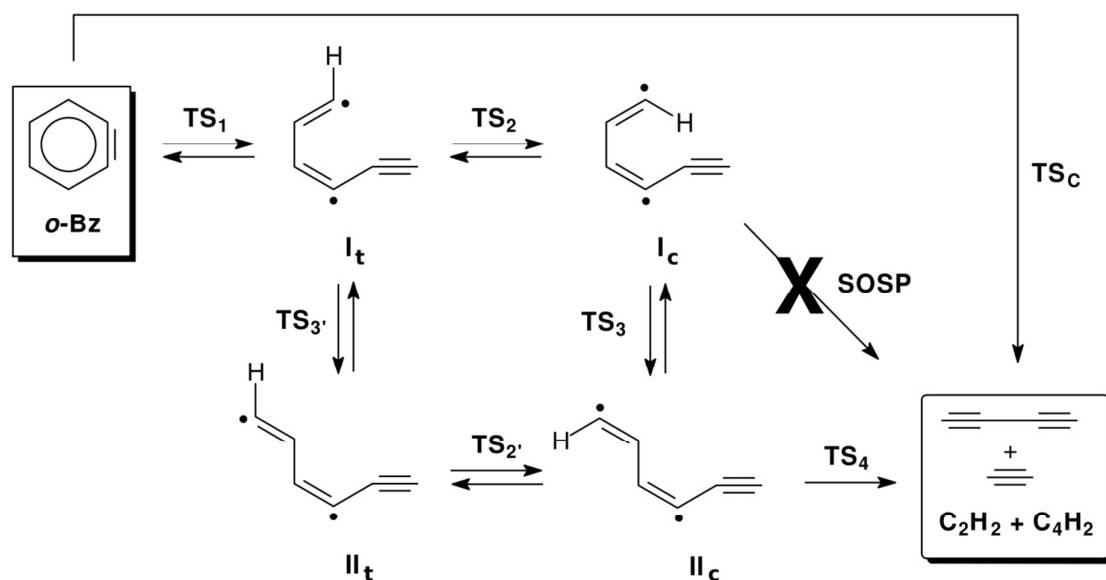
Scheme 1. Concerted *vs.* stepwise fragmentation pathways of *o*-benzyne.

The stepwise diradical pathway is slightly energetically preferred with respect to the concerted one (through **TS$_C$**). This is also evident if we include in our energy data the effect of temperature and entropy; both transition structures **TS$_C$** and **TS$_1$** are favored by entropy: at 600 K, for instance, the ΔS values are 13.0 and 13.8 cal mol^{-1} K^{-1}, respectively (the value reported[22] for **TS$_C$** at 500 K is 16.3 cal mol^{-1} K^{-1}). Figure 2 shows the free energy profiles at some selected temperatures for the two competing fragmentation processes. It is evident that the stepwise reaction always shows a lower energy profile but the difference is never very high (5-6 kcal mol^{-1}). Two other observations can be made: the fragments becomes thermodynamically favored above 1200K and the first transition structure (**TS$_1$**) is the rate determining step in the stepwise pathway. Both pathways, through the two transition structures **TS$_C$** and **TS$_1$** will be included in the kinetic analysis.
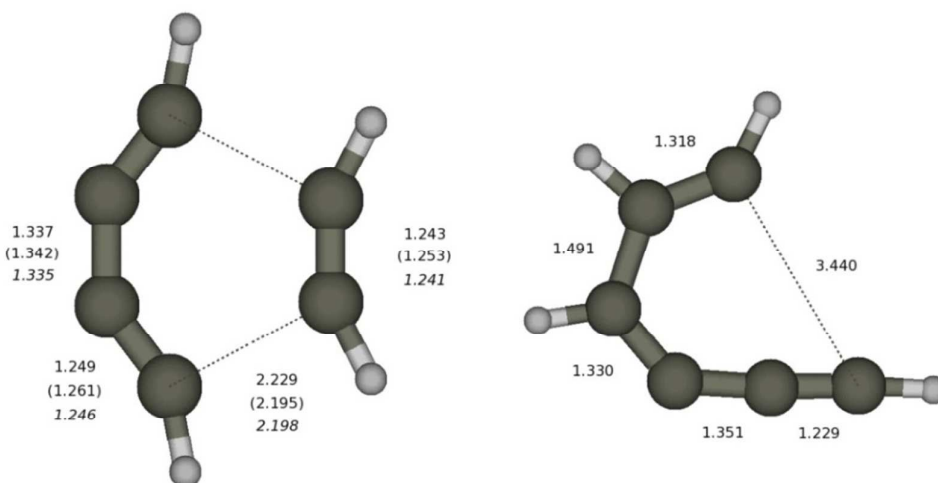
Figure 1. Transition structures for the concerted (**TS$_C$**, left) and stepwise (**TS$_1$**, right) fragmentation pathways of *o*-benzyne. Distances in Å. Plain values are CAS(12,12)-PT2/ cc-pVTZ; values in parenthesis are MP2/6-31G(d) from ref. 34; values in italics are CCSD(T)-AE/cc-pCVQZ from ref. 35.
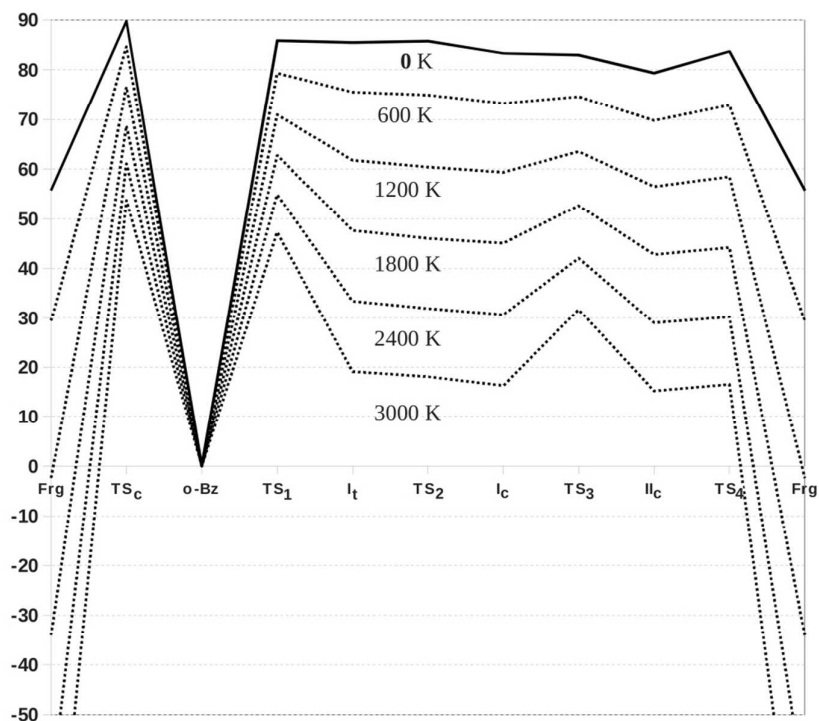
Figure 2. Free energy profiles (in kcal mol^{-1}) for the concerted (left) and the stepwise (right) fragmentation pathways of *o*-benzyne.

Table 1. Relative internal energy (E+ZPE, kcal mol^{-1}) for fragmentations of *o*-benzyne.

Structures	ΔE^a	ΔE^b	ΔE^c
o-benzyne	0.0	0.0	0.0
TS$_c$	89.7	89.7	89.8
TS$_1$	84.3	85.2	85.9
I$_t$	83.5	84.6	85.5
TS$_2$	84.8	85.4	85.8
I$_c$	81.4	82.5	83.3
TS$_3$	81.4	82.3	83.0
TS$_{3'}$	85.3	86.4	87.1
II$_t$	80.9	82.1	82.9
TS$_{2'}$	82.0	82.9	83.5
II$_c$	77.5	78.6	79.3
TS$_4$	82.7	83.3	83.7
C$_2$H$_2$ + C$_4$H$_2$	55.0	55.4	55.7

[a] Optimized CAS(12,12)-PT2/cc-pVTZ + ZPE$_{CASSCF}$; [b] single point CAS(12,12)-PT2/cc-pVQZ + ZPE$_{CASSCF}$. [c] CAS(12,12)-PT2/CBS + ZPE$_{CASSCF}$.

Isomerization of *o*-benzyne. As an alternative to the irreversible fragmentation to C_2H_2 + C_4H_2 through **TS$_1$** and **TS$_C$** (reported again in Scheme 2 and Table 2), *o*-benzyne can follow other fragmentations and isomerization pathways. We find the irreversible fragmentation suggested by Xu *et al.*[36] and consisting in hydrogen loss (**TS$_5$**, 106.8 kcal mol^{-1}) that yields the high energy triradical intermediate 1,2,3-tridehydrobenzene **III** (106.8 kcal mol^{-1}). The alternative hydrogen loss yielding to 1,2,4-tridehydrobenzene was not considered because energetically ~~even more~~ unfavorable: the 1,2,4 isomer is estimated[42] to be 8 kcal mol^{-1} above the 1,2,3 isomer and therefore is not included in this scheme.

The most important isomerization of *o*-benzyne converts it (**TS$_6$**, 69.4 kcal mol^{-1}) in its *meta* isomer (12.3 kcal mol^{-1}). These energy values are in good agreement with those (69.4 and 12.5) calculated by Sander *et al.*[40] Indeed, this process goes through the formation of cyclopentadienylidene (located at 29.9 kcal mol^{-1}) whose stability is extremely low: the CASPT2/QZ activation energy for its back-rearrangement to *o*-benzyne is only 1.4 kcal mol^{-1} (see the Supporting Information for more details and figure 7 in ref. 41). Therefore, this specie is ignored and **TS$_6$** is taken as unique critical point in our scheme and in the forthcoming kinetic treatment. Anyway, cyclopentadienylidene is supposed to be important in the scrambling of the position of the "triple bond" in *o*-benzyne.[43]

Once formed, *m*-benzyne can rearrange (**TS$_7$**, 64.3 kcal mol^{-1}) to *cis*-hexa-3-en-1,6-diyne (*cis*-HED, 19.3 kcal mol^{-1}). The Sander *et al* energy values[40] are 59.7 and 14.7 kcal mol^{-1}, respectively. *cis*-HED can evolve though three pathways: the cyclization (**TS$_8$**, 46.6 kcal mol^{-1}) to *p*-benzyne (28.3 kcal mol^{-1}); the *cis-trans* isomerization (**TS$_9$**, 68.4 kcal mol^{-1}) to *trans*-hexa-3-en-1,6-diyne (*trans*-HED, 19.1 kcal mol^{-1}); the irreversible hydrogen loss (**TS$_{12}$**, 119.3 kcal mol^{-1}) to the radical **IV** (119.4 kcal mol^{-1}). The energy values obtained by Sander *et al* [40] for the first pathway are 44.3 and 26.6 kcal mol^{-1}. This pathway is the well-known *Bergman* cyclization described by Jones and Bergman in 1972[44] and subject of several computational works.[45] The calculated energy barrier (27.3 kcal mol^{-1}) and reaction energy (9.0 kcal mol^{-1}) for this reaction (both making reference to *cis*-HED) are in good agreement with the experimental values of 28-32 and 8-14 kcal mol^{-1}, respectively.[44,46,47] The other two pathways (through **TS$_9$** and **TS$_{12}$**) have not been considered previously in any other work. For *trans*-HED two irreversible reactions are possible: the hydrogen loss (**TS$_{11}$**, 119.1 kcal mol^{-1}) to the radical **IV** and the fragmentation (**TS$_{11}$**, 99.3 kcal mol^{-1}) to C_2H_2 + C_4H_2. Radical **IV**, irreversibly generated from the two HED isomers is expected[36] to easily lose a second hydrogen atom yielding C_6H_2. The alternative but energetically unfavorable mechanisms for the *ortho*- to *m*-benzyne and *meta*- to *p*-benzyne isomerizations consisting in hydrogen [1,2]-migrations previously identified[34,40] were not explored in this work.
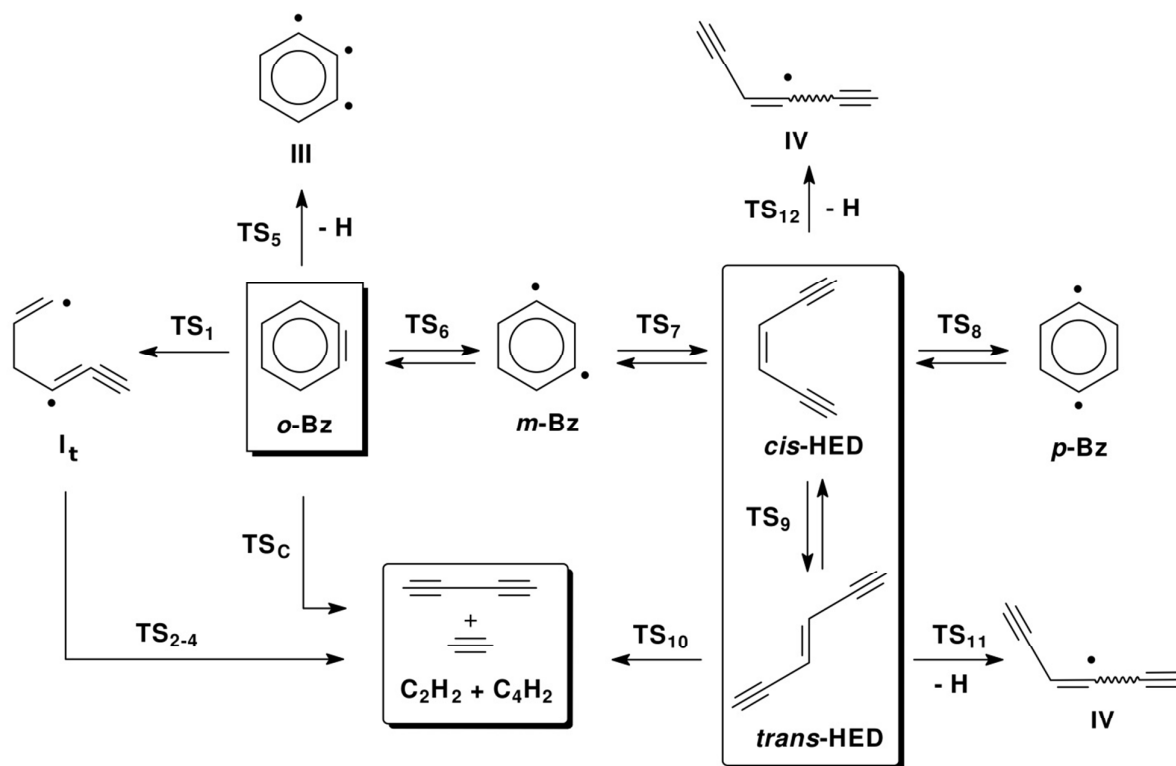
Scheme 2. Isomerization and fragmentation pathways of *o*-benzyne.

Table 2. Relative internal energy (E+ZPE, kcal mol^{-1}) for fragmentations and isomerizations of *o*-benzyne.

Structures	ΔE^a	ΔE^b	ΔE^c
o-benzyne	0.0	0.0	0.0
TS$_c$	89.7	89.7	89.8
TS$_1$	84.3	85.2	85.9
TS$_5$	106.6	106.7	106.8
III	104.6	105.2	105.8
TS$_6$	69.8	69.6	69.4
m-benzyne	11.8	12.1	12.3
TS$_7$	63.2	63.8	64.3
cis-HED	18.9	19.2	19.3
TS$_8$	46.0	46.3	46.6
p-benzyne	27.1	27.8	28.3
TS$_9$	67.2	67.9	68.4
trans-HED	18.5	18.9	19.1
TS$_{10}$	97.9	98.7	99.3
TS$_{11}$	117.2	118.3	119.1
TS$_{12}$	117.5	118.5	119.3
IV + H	117.4	118.6	119.4
C$_2$H$_2$ + C$_4$H$_2$	55.0	55.4	55.7

^{a} Optimized CAS(12,12)-PT2/cc-pVTZ + ZPE$_{CASSCF}$; ^{b} single point CAS(12,12)-PT2/cc-pVQZ + ZPE$_{CASSCF}$; ^{c} CAS(12,12)-PT2/CBS + ZPE$_{CASSCF}$

Thermal decomposition of *o*-benzyne

The calculated energies and partition functions for the fragmentation and isomerization pathways described above have been treated with the Transition State Theory to get the kinetic rate constants illustrated in Figure 3 (a table with all rate constants in reported in the Supporting Information).
Above ca. 900 K, we can see that $k_{cis\text{-}HED}$ (calculated as $(k_6 \, k_7)/k_{-6}$), which corresponds to the rate constant for the isomerization of *o*-benzyne to *cis*-HED passing through *m*-benzyne, becomes important (greater than 1 s^{-1}). The [*cis*-HED]/[*o*-benzyne] equilibrium constant, illustrated by $K_{cis\text{-}HED}$ (calculated as $(k_6 \, k_7)/(k_{-6} \, k_{-7})$) become thermodynamically favored (> 1) above 1200K. The isomerization of *cis*-HED to *trans*-HED is also very fast (k_9). The k_9/k_{-9} ratio (not shown), is the [*trans*-HED]/[*cis*-HED] equilibrium constant which is always close to 1 (k_{-9}, not shown, is always slightly smaller than k_9) and in favor of the *trans* isomer.

Therefore, above 900-1000 K o-benzyne will first isomerize to both HEDs isomers. Between 1200-1300 K all rate constants go beyond 1 s^{-1}. Several rate constants are grouped together:~~, these are~~ the rate constants for the formation of C_2H_2 + C_4H_2 through the fragmentation reactions of o-benzyne (k_C for the concerted and k_1 for the stepwise) and from $trans$-HED (expressed by $k_{frags} = (k_6\ k_7\ k_9\ k_{10})\ /(k_{-6}\ k_{-7}\ k_{-9})$); the hydrogen loss from o-benzyne yielding the triradical **III** (k_5); the rate constant for the formation of **IV** from $trans$-HED (expressed by $k_{IV\ trans} = (k_6\ k_7\ k_9\ k_{11})\ /(k_{-6}\ k_{-7}\ k_{-9})$). The rate constant for the formation of **IV** from cis-HED (expressed by $k_{IV\ cis} = (k_6\ k_7\ k_{12})\ /(k_{-6}\ k_{-7})$) follows a different trend.

Other equilibrium constants, calculated as ratios between rate constants, are also indicative: $K_{m\text{-}bz}$ (calculated as k_6/k_{-6}), which corresponds to the [m-benzyne]/[o-benzyne] equilibrium and K_B (calculated as k_8/k_{-8}) , which corresponds to the [p-benzyne]/[cis-HED] equilibrium. $K_{m\text{-}bz}$ becomes greater than 1only at high temperature (above 2400 K) while K_B is always significantly lower. Therefore the accumulation of the $meta$ and $para$ isomers of benzyne is expected to be very improbable.
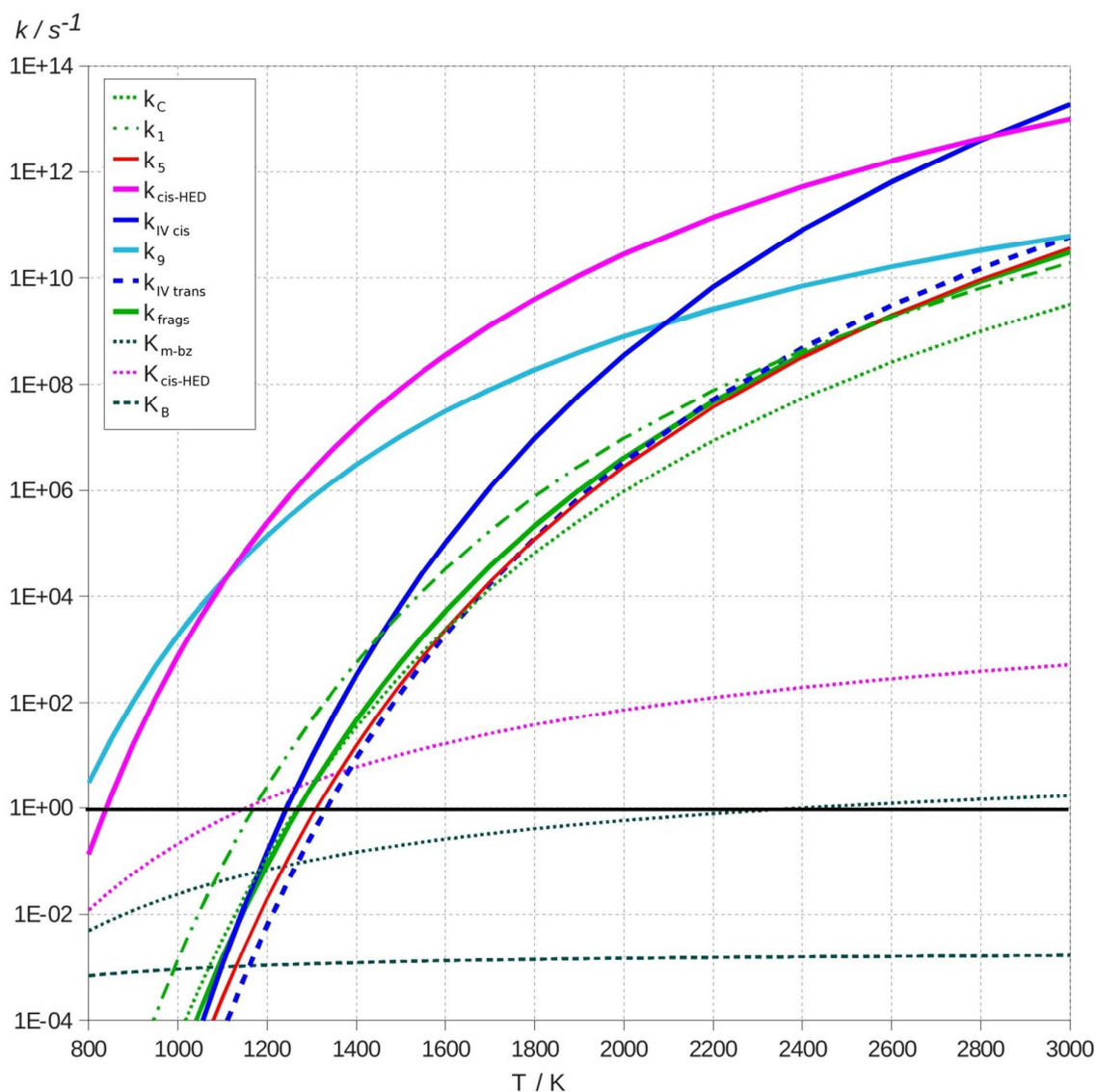
Figure 3. Rate constants (s^{-1}) for isomerization and fragmentation pathways of o-benzyne.
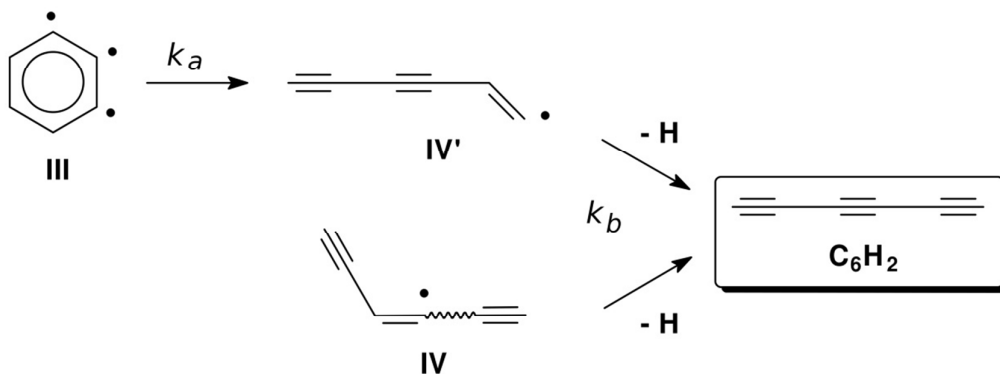
Scheme 3. Formation of C_6H_2 through isomerization and fragmentation of radicals **III** and **IV**s.

Intermediates **III** and **IV** undergo other transformations (Scheme 3). The triradical **III** first isomerizes[36] to the open chain radical **IV'** which then loses a second hydrogen atom yielding C_6H_2. This product is obtained also from the radical **IV** though an analogue H-loss.

Table 3. Rate constants (s^{-1}) for the formation of C_6H_2 through the isomerization and fragmentation of radicals **III** and **IV** (see Scheme 3). $k = A \exp(-E_a/RT)$; E_a in kcal mol^{-1}.

Structures	A	E_a
k_a	4.8 x 10^{10}	98.2
k_b	2.3 x 10^{10}	53.7

The rate constants calculated in the present work (see Scheme 2 and Figure 3) and the rate constant taken from ref. 36 (Table 3) for the reactions shown in Scheme 3 have been used to model the *o*-benzyne rearrangement and fragmentation at several temperatures. Further fragmentation reactions starting from C_2H_2, C_4H_2 and C_6H_2 and reactions involving the hydrogen atoms generated as in Scheme 2 are not included in the present model since their study is beyond the scope of this work. Most representative profiles of yield(%) *vs.* time are reported (Figure 4) and commented for six different temperatures.

At 1000 K and within 2 sec the concentration of *o*-benzyne decreases to 70% in equilibrium with the two isomers of HED.

At 1200 K the concentration of *o*-benzyne decreases to 25% in ca. 25 msec forming the two isomers of HED. At longer elapsed time, *trans*-HED (in fast equilibrium with *cis*-HED) slowly decomposes to C_2H_2 + C_4H_2 while *o*-benzyne continues to convert to HEDs until disappearance. At this temperature, very small amounts of both HEDs can also decompose to radical **IV** which immediately decomposes to C_6H_2 through H-loss.

At 1400 K the concentration of *o*-benzyne decreases to less than 10% in ca. 0.25 msec forming the two isomers of HED (ca 82% the sum of yields). Then *trans*-HED slowly decomposes to C_2H_2 + C_4H_2 while *o*-benzyne continues to convert to HEDs. At this temperature, both HEDs also decompose to radical **IV** which immediately decomposes to C_6H_2.
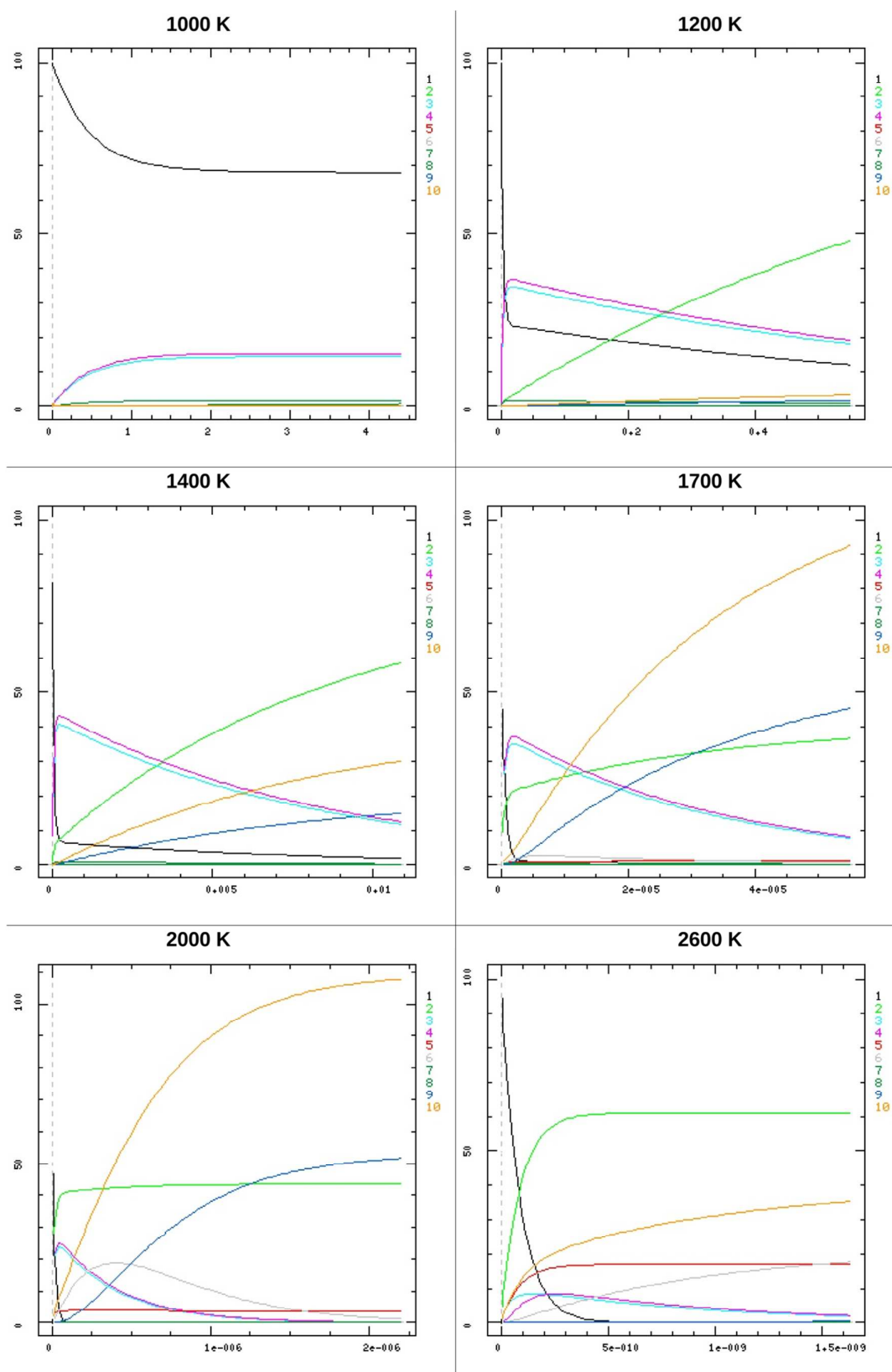
Figure 4. Calculated profiles of yield(%) vs. time(sec) for the thermal decomposition of *o*-benzyne at 1000, 1200, 1400, 1700, 2000 and 2600 K. **1**, *o*-benzyne; **2**, C_2H_2 + C_4H_2; **3**, *cis*-HED; **4**, *trans*-HED; **5**, **III**; **6**, **IV+IV'**; **7**, *m*-benzyne; **8**, *p*-benzyne; **9**, C_6H_2; **10**, hydrogen atoms.

At 1700 K o-benzyne disappears within 2 μsec forming the two isomers of HED (70% the sum). In the same time, a 22% of C_2H_2 + C_4H_2 seems to form directly from o-benzyne while other forms from fragmentation of $trans$-HED. The decomposition (through **IV**) of both isomers of HED yields C_6H_2 whose formation, if a longer time is allowed to elapse, prevails on the formation of C_2H_2 + C_4H_2.

At 2000 K o-benzyne disappears within 50 nsec fragmenting to C_2H_2 + C_4H_2 (40% ca) and forming the two isomers of HED (50% the sum). Then C_2H_2 + C_4H_2 continue to form from $trans$-HED and the decomposition of both isomers of HEDs yields C_6H_2 which prevails at long time. For a short time (a few μsec), small amounts of **III** and **IV** accumulate.

At 2600 K o-benzyne disappear within 0.5 nsec fragmenting mainly to C_2H_2 + C_4H_2 (60% ca) and, to a lesser extent, to **III** (18%) and HEDs (18% the sum). Then **III** isomerizes to **IV'** (summed into **IV** in the profiles) that later forms C_6H_2.

At some temperatures, we can also see that very small amounts of m-benzyne accumulates only for a short time because it isomerizes to the more stable cis-HED, while p-benzyne barely appears. This was already expected from the inspection of the equilibrium constants (see above) and it is coherent with the observation that in experiments of flash vacuum pyrolysis m- and p-benzyne are unstable and both rearrange to HED.[48,49] This phenomenon can be explained with the fact that they are less stable than their $ortho$ isomer and they suffer from an unfavorable entropy term with respect to the two hexa-3-en-1,6-diyne. m-Benzyne is slightly more stable than the two HED isomers (ca. 7 kcal mol^{-1}), however, the latter take advantage of a favorable entropy factor (TΔS) which is estimated (at 2400 K when the two HED isomers reach the maximum yield) to be 13-15 kcal mol^{-1}.

The formation and the decomposition of **III**, **IV** and **IV'** also yield hydrogen atoms which clearly appear above 1400 K.

It is evident from the profiles just seen that the final products of the thermal decomposition of o-benzyne, cis and $trans$ HED, C_2H_2 + C_4H_2, and C_6H_2, form in different amounts depending on temperature and time. Figure 5 shows the relative yields of these product in the range 800-3000 K at 50 μsec (typical interval used in experiment[19,22,36]) and at 5 sec, a time long enough to find all processes finished (yield profiles at 50nsec, 5 and 500 μsec and 50 msec of elapsed time are reported in the Supporting Information).

After 50 μsec o-benzyne is stable up to 1200 K, above this temperature it starts to decompose. At 1700 K there is no o-benzyne left. Between 1200 and 1800 K, the two isomers of HED are the main products. They reach the maximum yields (ca 40% each) at 1500 K. Above 1800 K their decomposition is complete before than 50 μsec. Figure 6 shows the time at which $trans$-HED (the more stable) reaches the maximum yield at different temperatures. Not surprisingly, the higher the temperature, the shorter the time $trans$-HED appears. Above 1400 K, C_2H_2 + C_4H_2 appear while C_6H_2 appears at 1600 K. The two yield profiles crosses twice: these is an effect of the different sources and mechanisms that we have already discussed above. Anyway, above 1800 K and after 50 μsec C_2H_2, C_4H_2 and C_6H_2 are the only species left.

After 5 sec and above 1200 K, o-benzyne is fully decomposed. Smalls amount of cis and $trans$-HED (ca 20% each) can be found between 900 and 1200K. Between 1000 and 1600 K, the yield of C_2H_2 + C_4H_2 shows a

maximum (97 % at 1200 K) then the yield decay oscillating between 40 and 60 % above 1400 K. The yield of C_6H_2 starts to grow from 1200 K and reaches a maximum at 1800 K (ca 60%) then is stabilizes around 40 % above 1800 K.
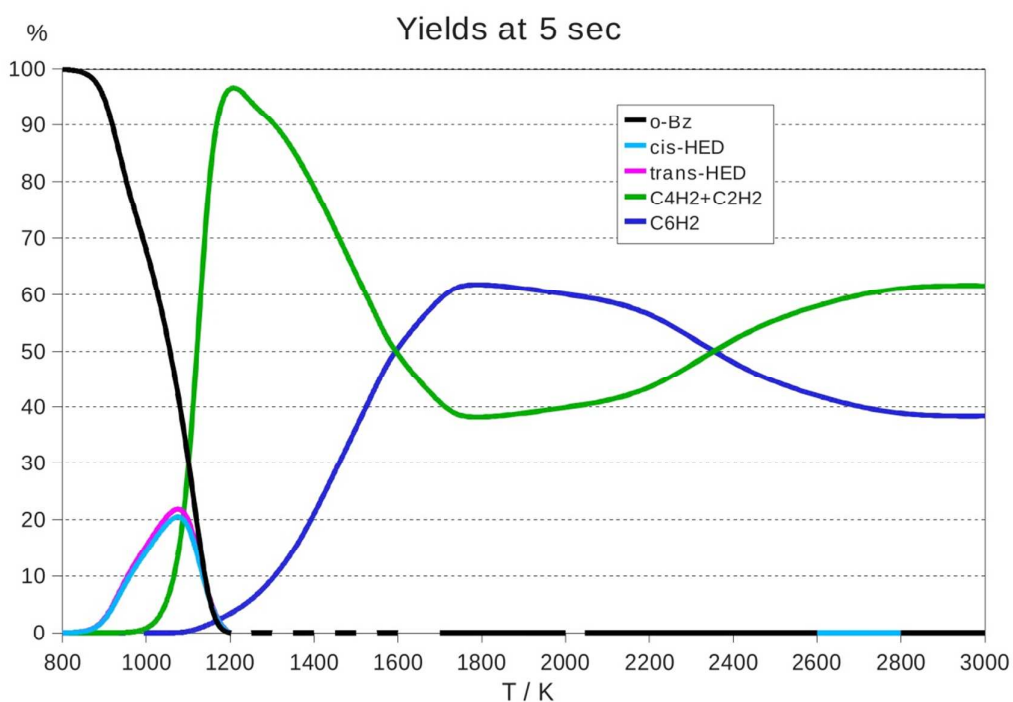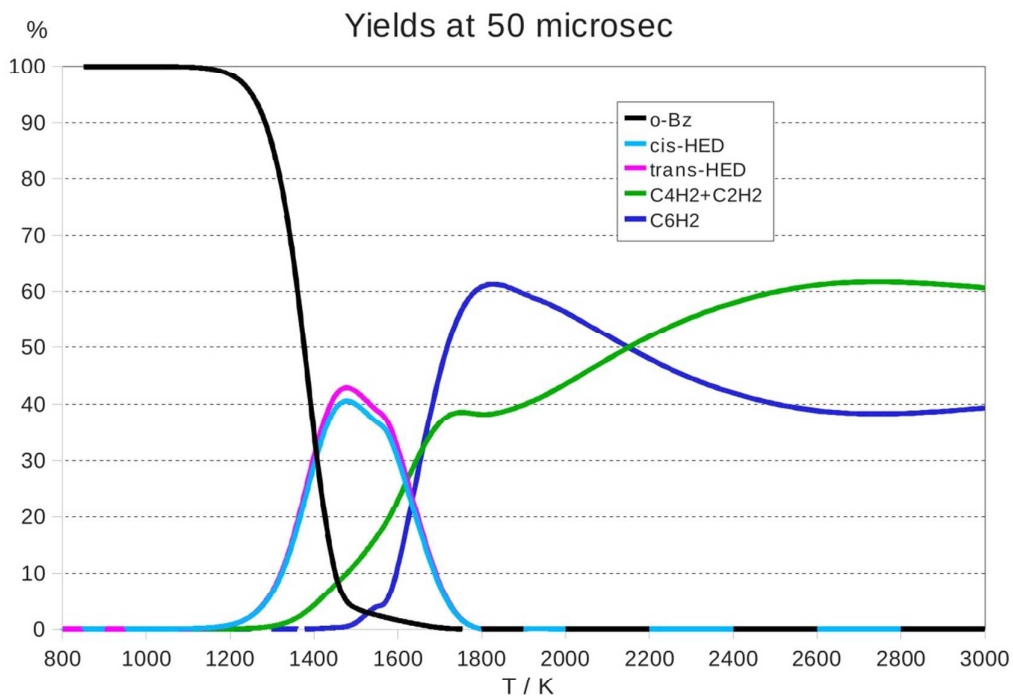
Figure 5. Calculated yield(%) vs. temperature for the thermal decomposition of *o*-benzyne.
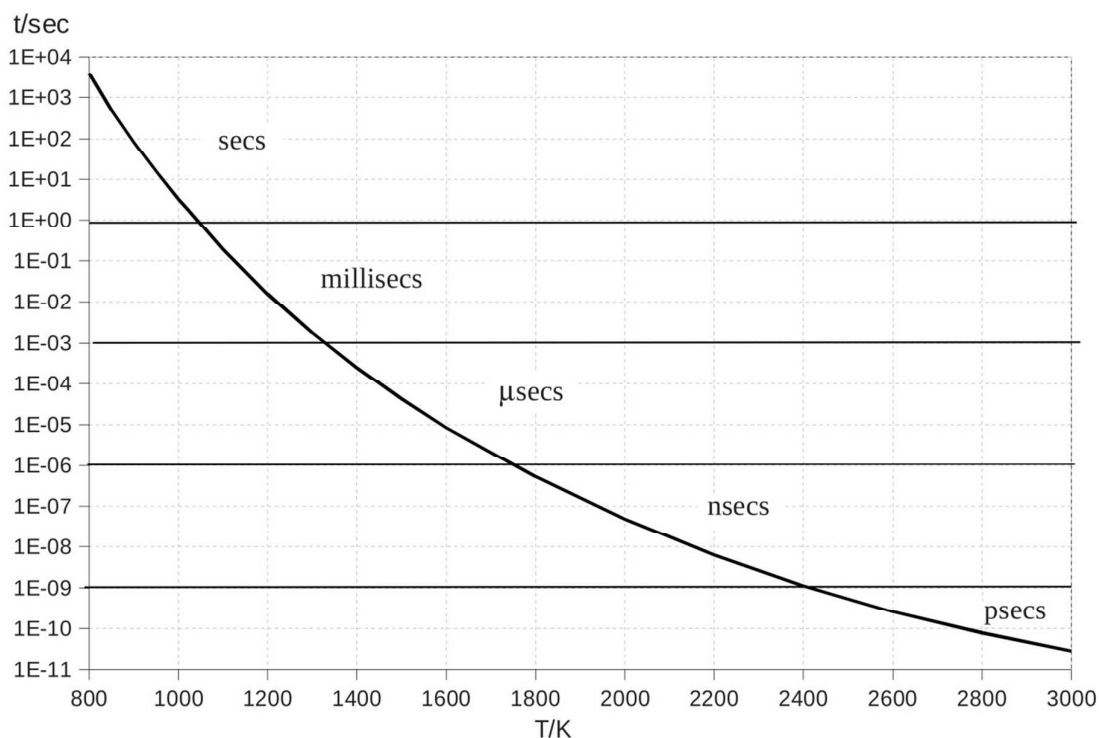
Figure 6. Elapsed time to reach *trans*-HED maximum in the decomposition of *o*-benzyne.

Conclusions

The thermal decomposition of *o*-benzyne is predicted to yield C_2H_2, C_4H_2 and C_6H_2 as main products. In detail: *o*-benzyne first isomerizes to *cis*-hexa-3-en-1,6-diyne (HED) that rapidly equilibrates with its slightly more stable *trans* isomer. However, only small amounts of HEDs accumulate because they rapidly decompose to C_2H_2, C_4H_2 and C_6H_2 (the latter only above 1200 K). Between 1000 and 1400 K, $C_2H_2 + C_4H_2$ form exclusively from decomposition of *trans*-HED. Above 1400 K, $C_2H_2 + C_4H_2$ also form from direct fragmentation of *o*-benzyne. The fragmentation through radical **IV** of *cis* and *trans*-HED yields C_6H_2. The competition between the two fragmentation pathways of the two isomer of HED (to $C_2H_2 + C_4H_2$ from the *cis* isomer only and to C_6H_2 from both isomers) sees the one leading to $C_2H_2 + C_4H_2$ to prevail between 1000 and 1600 K and the one leading to C_6H_2 to prevail above 1600 K. However, above 2400 K, the direct fragmentation of *o*-benzyne causes the formation of to $C_2H_2 + C_4H_2$ to prevail, again. At high temperature (above 2400 K) the fragmentation of *o*-benzyne to **III** (which finally gives C_6H_2) shows some minor role. Although in our model several collateral reactions have not been included we can observe some point of agreement with the experiments: i. C_2H_2 and C_4H_2 are the main products; ii. *cis*- and *trans*-hexa-3-en-1,6-diyne are formed but do not accumulate (except in a small range of lower temperatures) and this explain why they have not been observed in some experiments;[35] iii. starting from 1400 K our model predicts the formation of hydrogen atoms as experimentally observed.[19,22,36]

Computational method

All geometries have been optimized and characterized by vibrational analysis at the CAS(12,12)-SCF[50,51,52] level with the cc-pVTZ basis set.[53] The active space, making reference to o-benzyne, includes the full π system (6 electrons in 6 orbitals) plus the electrons and the orbitals of the in-plane "π" bond (2,2) plus two couples of electrons and orbitals (4,4) related to the CC σ bonds involved in the fragmentations or in the rearrangements. In H-losses TSs the (2,2) subset of one of the CC σ bond not involved in the reaction is substituted with the (2,2) subset of the CH σ bond involved in the fragmentations. The second-order perturbation treatment, which include all orbitals, reduces the energy difference due to the difference in the composition of the active spaces (that are always 12 electrons in 12 orbitals) to 1 kcal mol^{-1}. Active orbitals transform in π orbitals in C_4H_2 and C_2H_2. Pictures of all active molecular orbitals and relative occupation number for all structures are reported in the Supporting Information.. CASSCF calculations are also used to generate the ZPE which are scaled by 0.93 (see the Supporting Information for more details). Geometries have been reoptimized at the CAS(12,12)-PT2 level[54,55,56] with the same basis set. This computational approach recovers both the dynamic and non-dynamic correlation energies and it is the only method suitable for a correct and homogenous treatment of the electronic structure of all species. The CASPT2 calculations have been performed by taking advantage of the Cholesky decomposition of the two-electron integrals.[57,58,59] Energies have been recalculated by single-point calculation with the cc-pVQZ basis set.[53] Then the CASPT2/CBS (E_{CBS}, complete basis set) energies have been obtained from the CASPT2/cc-pVTZ (E_3) and CASPT2/cc-pVQZ (E_4) energy values through the extrapolation formula put forward by Halkier *et al*.:[60] $E_{CBS} = (E_3 3^3 - E_4 4^3)/(3^3 - 4^3)$. Finally, the CASPT2/CBS energies have been combined with the ZPVE calculated at the CASSCF/cc-pVTZ level to get the E_{ZPVE} reported in Tables and throughout in the text. Quantum chemical calculations have been performed by the program MOLCAS 7.4[61] The reaction rate constants have been used in the kinetic modelling program DynaFit.[62] Figure 1 and molecular orbital pictures in the Supporting Informations have been obtained with the graphical program Molden.[63]

Bibliography

1. C. Wentrup, *Aust. J. Chem,.* 2010, **63**, 979-986.

2. W. E. Bachmann, H. T. Clarke, *J. Am. Chem. Soc.,* 1927, **49**, 2089-2098.

3. O. L. Chapman, K. Mattes, C. L. McIntosh, J. Pacansky, G.V. Calder, G. Orr, *J. Am. Chem. Soc.,* 1973, *95*, 6134-6135.

4. I. R. Dunkin, J. G. MacDonald, *J. Chem. Soc., Chem. Commun.,* 1979, 772-773.

5. G. Doreen, A. E. S. Leopold, W. C. Miller, *J. Am. Chem. Soc,.* 1986, **108**, 1379-1384.

6.   C. Wentrup, R. Blanch, H. Briehl, G. Gross, *J. Am. Chem. Soc.,* 1988, **110**, 1874-1880.

7.   J. G. Radziszewski, B. A. Hess, Jr., R. Zahradnik, *J. Am. Chem. Soc.* 1992, **114**, 52-57.

8.   H. F. Bettinger, P. v. R. Schleyer, H. F. Schaefer, III, *J. Am. Chem. Soc.* 1999, **121**, 2829-2835.

9.   S. G. Kukolich, C. Tanjaroon, M. C. McCarthy, P. Thaddeus, *J. Chem. Phys.* 2003, **119**, 4353-4359.

10. S. G. Kukolich, M. C. McCarthy, P. Thaddeus, *J. Phys. Chem. A* 2004, **108**, 2645-2651.

11. P. Groner, S. K. Kukolich, *J. Mol. Struct.* 2006, **780-781**, 178-181

12. P. D. Godfrey, *Aust. J. Chem.* 2010, **63**, 1061-1065.

13. C. W. Bauschlicher Jr., A. Ricca, *Chem. Phys. Letters* 2013, **566**, 1-3.

14. K. J. Cahill, A. Ajaz, A., R. P. Johnson, *Aust. J. Chem.* 2010, **63**, 1007-1012 and reference therein.

15. H. H. Wenk, M. Winkler, W. Sander, *Angew. Chem. Int. Ed.* 2003, **42**, 502-528.

16. H. Pellissier, M. Santelli *Tetrahedron* 2003, **59**, 701-730.

17. A. V. Dubrovskiy, N. A. Markina, R. C. Larock, *Org. Biomol. Chem.* 2013, **11**, 191-218.

18.   V. S. Rao, G. B. Skinner, *J. Phys. Chem.* 1984, **88**, 5990-5995.

19. J. H. Kiefer, L. J. Mizerka, M. R. Patel, H.-C. Wei, *J. Phys. Chem.* 1985, **89**, 2013-2019.

20. H. Wang, M. Frenklach *J. Phys. Chem.* 1994, **98**, 11465-11489.

21. L. K. Madden, L. V. Moskaleva, S. Kristyan, M. C. Lin, *J. Phys. Chem. A* 1997, **101**, 6790-6797.

22. H. Wang, A. Laskin, N. W. Moriarty, M. Frenklach, *Proc. Combust Inst.* 2000, **28**, 1545-1555.

23. R. S. Tranter, S. J. Klippenstein, L. B. Harding, B. R. Giri, X. Yang, J. H. Kiefer, *J. Phys. Chem. A* 2010, **114**, 8240-8261.

24. S. H. Duerrstein, M. Olzmann, J. Aguilera-Iparraguirre, R. Barthel, W. Klopper, *Chem. Phys. Lett.* 2011, ***513***, 20-26.

25. H. Ricter, T. G. Benish, O. A. Mazyar, W. H. Green, J. B. Howard, *Proc. Combust Inst.* 2000, **28**, 2609-2618.

26. B. Shukla, K. Tsuchiya, M. Koshi *J. Phys. Chem. A* 2011, **115**, 5284-5293.

27. A. Comandini, K. J. Brezinsky, *J. Phys. Chem. A* 2011, **115**, 5547-5559.

28. A. Comandini, K. J. Brezinsky, *J. Phys. Chem. A* 2012, **116**, 1183-1190.

29. A. Comandini, T. Malewicki, K. J. Brezinsky, *J. Phys. Chem. A* 2012, **116**, 2409-2434.

30. A. Matsugi, A. Miyoshi, *Phys. Chem. Chem. Phys.* 2012, **14**, 9722-9728.

31. S. L. W. Weaver, A. J. Remijan, R. J. McMahon, B. J. McCall *Astrophys. J.* 2007, **671**, L153-L156.

32. F. Zhang, D. Parker, I. S. Kim, R. I. Kaiser, A. M. Mebel, *Astrophys. J.* 2011, **728**, 1-10.

33. W.-Q. Deng, K.-L. Han, J.-P. Zhan, G.-Z. He, *Chem. Phys. Letters* 1988, **288**, 33-36.

34. L. V. Moskaleva, L. K. Madden, M. C. Lin, *Phys. Chem. Chem. Phys.* 1999, **1**, 3967-3972.

35. X. Zhang, A. T. Maccarone, M. R. Nimlos, S. Kato, V. M. Bierbaum, G. B. Ellison, B. Ruscic, A. C. Simmonett, W. D. Allen, H. F. Schaefer III, *J. Chem. Phys.* 2007, **126**, Art. 044312.

36. C. Xu, M. Braun-Unkhoff, C. N. Frank, *Proceedings Comb. Inst.* 2007, **31**, 231-239.

37. A. Ajaz, A. Z. Bradley, R. C. Burrell, W. H. Li, K. J. Daoust, L. B. Bovee, K. J. DiRico, R. P. Johnson, *J. Org. Chem.* 2011, **76**, 9320-9328.

38. We must report that Zhang *et al.* suggested the possible existence of an alternative stepwise channel (ref. 35).

39. W. Sander, M. Exner, M. Winkler, A. Balster, A. Hjerpe, E. Kraka, D. Cremer, *J. Am. Chem. Soc.* 2002, **124**, 13072-13079.

40. M. Winkler, B. Cakir, W. Sander, *J. Am. Chem. Soc.* 2004, **126**, 6135-6149.

41. W. Wichael, W. Sander, *Aust. J. Chem.* 2010, **63**, 1013-1047.

42. D. J. Goebbert, P. G.Wenthold, *Int. J. Mass Spectrom.* 2006, **257**, 1-11.

43. R. F. C. Brown, *Eur. J. Org. Chem.* 1999, 3211-3222.

44. R. R. Jones, R. G. Bergman, *J. Am. Chem. Soc.* 1972, **94**, 660-661.

45. H. Dong,B.-Z. Chen, M.-B. Huang,R. Lindh *J. Comput. Chem.* 2012, **33**, 537–549 and references therein.

46. W. R. Roth, H. Hopf, C. Horn, *Chem. Ber.* 1994, **127**, 1765-1779.

47. P. Wenthold, R. R. Squires, *J. Am. Chem. Soc.* 1994, **116**, 6401-6412.

48. I. P. Fisher, F. P. Lossing, *J. Am. Chem. Soc.* 1963, **85**, 1018-1019.

49. W. Sander, *Acc. Chem. Res.* 1999, **32**, 669-676.

50. P.-Å. Malmqvist,; A. Rendell, B. O. Roos, *J. Phys. Chem.* 1990, **94**, 5477-5482.

51. B. O. Roos, P. R. Taylor, P. E. M. Siegbahn, *Chem. Phys.* 1980, **48**, 157-173.

52. B. O. Roos, *Advances in Chemical Physics*; Ab Initio Methods in Quantum Chemistry (Ed.: K. P. Lawley), John Wiley & Sons Ltd., Chichester, 1987, vol. II, chapter 69.

53. T.H. Dunning, Jr., *J. Chem. Phys.* 1989, **90**, 1007-1023.

54. K. Andersson, P.-Å. Malmqvist, B. O. Roos, A. J. Sadley, K. Wolinski, *J. Phys. Chem.* 1990, **94**, 5483-5488.

55. K. Andersson, P.-Å. Malmqvist, B. O. Roos, *J. Phys. Chem.* 1992, **96**, 1218-1226.

56. G. Ghigo, B. O. Roos, P.-Å. Malmqvist, *Chem. Phys. Lett.* 2004, **396**, 142-149.

57. H. Koch, A. S. de Merás, T. B. Pedersen, *J. Chem. Phys.* 2003, **118**, 9481-9484.

58. F. Aquilante, P.-Å. Malmqvist, T. B. Pedersen, A Ghosh, B. O. Roos, *J. Chem. Theor. Comput.* 2008, **4**, 694-702.

59. F. Aquilante, T. B. Pedersen, R. Lindh, *J. Chem. Phys.* 2007, **126**, Art. 194106.

60. A. Halkier, T. Helgaker, P. Jørgensen, W. Klopper, H. Koch, J. Olsen, A. K. Wilson, *Chem. Phys. Lett.* 1998, **286**, 243-252.

61. F. Aquilante, L. De Vico, N. Ferré, G.; Ghigo, P.-Å. Malmqvist, P. Neogrády, T. B. Pedersen, M. Pitoňák, M. Reiher, B. O. Roos; L. Serrano-Andrés, M. Urban, V. Veryazov, R. Lindh, *J. Comput. Chem.* 2010, **31**, 224-247.

62. P. Kuzmic, *Anal. Biochem.* 1996, **237**, 260-273.

63. G. Schaftenaar, J. H. Noordik, *J. Comput.-Aided Mol. Design* 2000, **14**, 123-134.